Biochemical and Biophysical Research Communications 460 (2015) 210–215

Contents lists available at ScienceDirect

Biochemical and Biophysical Research Communications

journal homepage: www.elsevier.com/locate/ybbrc

A new enzyme involved in the control of the stereochemistry in the decalin formation during equisetin biosynthesis

Naoki Kato [a], Toshihiko Nogawa [a], Hiroshi Hirota [a, b], Jae-Hyuk Jang [c], Shunji Takahashi [a, b], Jong Seog Ahn [c], Hiroyuki Osada [a, *]

[a] Chemical Biology Research Group, RIKEN Center for Sustainable Resource Science, Wako, Saitama 351-0198, Japan
[b] RIKEN-KRIBB Joint Research Unit, Global Research Cluster, RIKEN, Wako, Saitama 351-0198, Japan
[c] Chemical Biology Research Center, Korea Research Institute of Bioscience and Biotechnology (KRIBB), 30 Yeongudanji-ro, Ochang, Cheongwon, Chungbuk 363-883, Republic of Korea

ARTICLE INFO

Article history:
Received 12 February 2015
Available online 11 March 2015

Keywords:
Biosynthesis
Decalin
Diels-Alder cycloaddition
Fusarium PKS-NRPS hybrid
Secondary metabolite

ABSTRACT

Tetramic acid containing a decalin ring such as equisetin and phomasetin is one of the characteristic scaffolds found in fungal bioactive secondary metabolites. Polyketide (PKS)-nonribosomal peptide synthetase (NRPS) hybrid enzyme is responsible for the synthesis of the polyketide scaffold conjugated with an amino acid. PKS-NRPS hybrid complex programs to create structural diversity in the polyketide backbone have begun to be investigated, yet mechanism of control of the stereochemistry in a decalin formation via a Diels-Alder cycloaddition remains uncertain. Here, we demonstrate that *fsa2*, which showed no homology to genes encoding proteins of known function, in the *fsa* cluster responsible for equisetin and fusarisetin A biosynthesis in *Fusarium* sp. FN080326, is involved in the control of stereochemistry in decalin formation via a Diels-Alder reaction in the equisetin biosynthetic pathway.

1. Introduction

Fungal metabolites derived from polyketide synthase (PKS)-nonribosomal peptide synthetase (NRPS) hybrid enzymes such as fusarin C, tenellin, and equisetin are structurally complex and show a variety of biological activities [1,2]. The fungal PKS-NRPS hybrids are of particular interest because of their capability to synthesize diverse backbone structures [1,2]. Highly reducing PKS module synthesizes linear polyketide backbones, which are linked to an amino acid by the action of the NRPS module. Released products from the megasynthases are further converted to metabolites with more complex structures by tailoring enzymes, which are encoded by genes clustered with the megasynthase genes.

The Diels-Alder reaction, which is a [4+2] cycloaddition reaction to form a cyclohexene ring by the conjugation of a 1,3-diene to a dienophile [3], has been proposed as a key transformation process in some fungal PKS-NRPS hybrid pathways such as the equisetin, chaetoglobosin, and diaporthichalasin/phomopsichalasin pathways [4–6]. The involvement of Diels-Alderases in the formation of a decalin ring derived from similar highly-reducing PKS pathways has been demonstrated [7,8]. Lovastatin nonaketide synthase, LovB, catalyzes the Diels-Alder cycloaddition during the polyketide chain elongation to generate the proper stereochemistry for dihydromonacolin L [7]. It has been proposed that the enzyme-bound hexaketide intermediate is the actual substrate of LovB [9]. Solana-pyrone synthase (Sol5), a flavin-dependent oxidase, catalyzes the oxidation of prosolanapyrone II, which is a post-PKS product released from the prosolanapyrone synthase, Sol1, and the subsequent *exo*-specific cycloaddition reaction to yield solanapyrone A [8]. However, genes involved in a Diels-Alder reaction to form a decalin structure of equisetin (**1**) are yet to be identified.

Fusarisetin A (**2**), which was isolated as an acinar morphogenesis inhibitor, possesses a unique pentacyclic ring system [10] and has been proposed to be converted from **1**, since **2** contains the basic skeleton of **1** [11]. To establish the biosynthetic pathway for **2**, we conducted the genome mining of *Fusarium* sp. FN080326, a

Abbreviations: ATMT, *Agrobacterium tumefaciens*-mediated transformation; C6, $Zn(II)_2Cys_6$-type; ER, enoyl reductase; EtOAc, ethyl acetate; LC/ESI-MS, liquid chromatography/electrospray ionization mass spectrometry; MPLC, medium pressure liquid chromatography; MRM, multiple reaction monitoring; NRPS, nonribosomal peptide synthetase; PDB, potato dextrose broth; PKS, polyketide synthase; WT, wild type.

* Corresponding author. Chemical Biology Research Group, RIKEN Center for Sustainable Resource Science, 2-1 Hirosawa, Wako, Saitama 351-0198, Japan. Fax: +81 48 462 4669.
E-mail address: hisyo@riken.jp (H. Osada).

http://dx.doi.org/10.1016/j.bbrc.2015.03.011
0006-291X/

producer strain of **2**. In this study, we report that the *fsa* gene cluster is responsible for the biosynthesis of **1** and **2** in *Fusarium* sp. FN080326. A feeding experiment with the *fsa* gene deletion mutant showed that **1** is a biosynthetic intermediate of **2**. Furthermore, we identified a new gene, existing in some fungal PKS-NRPS hybrid gene clusters, that is involved in the stereocontrolled decalin formation of **1**.

2. Material and methods

2.1. Microbial strains

Fusarium sp. FN080326 was previously isolated [10]. *Rhizobium radiobacter* (*Agrobacterium tumefaciens*) C58 and the binary vector pBI121 were used for *A. tumefaciens*-mediated transformation (ATMT) of the fungus. *Escherichia coli* strain Stellar (Clontech, Mountain View, CA, USA) was used for plasmid construction and amplification.

2.2. Genome sequencing and gene prediction

The fungal genomic DNA of the strain FN080326 was extracted with the DNeasy Plant Mini kit (Qiagen, Hilden, Germany) and Genomic tip 20/G (Qiagen), and sequenced using Illumina HiSeq2000 (Illumina, San Diego, CA, USA) at the Genome Network Analysis Support Facility (GeNAS), RIKEN CLST, Yokohama, Japan. Sequence assembly was performed with CLC Genomics Workbench (CLC Bio, Aarhus, Denmark) to yield 820 contigs covering 40.2 Mb (Table S1). Gene annotation and prediction of secondary metabolite gene clusters were performed with the 2ndFind program (http://biosyn.nih.go.jp/2ndfind/).

2.3. Targeted gene inactivation

To construct the gene deletion plasmids, 2-kb DNA fragments upstream of the start codon and downstream of the stop codon of the target genes were amplified by PCR using chromosomal DNA of *Fusarium* sp. FN080326 as the template. The primer pairs, fsa-UF and -UR, and fsa-DF and -DR, were used for amplification of the upstream and downstream regions, respectively. The hygromycin B-resistant cassette (*hph*) was used as a selection marker [12]. These DNA fragments were combined in the original orientation in pBI121 in the following order: the upstream regions, *hph*, followed by the downstream regions (Fig. S1A). In-Fusion cloning system (Clontech) was used for the plasmid construction. The strain FN080326 was transformed with the resultant plasmids using the ATMT method as described previously [13]. Hygromycin B-resistant transformants (Δ*fsa*::*hph*) that resulted from a double-crossover between the deleted *fsa* sequence and the intact chromosomal *fsa* sequence were selected by culture in 50 μg/mL hygromycin B. Correct disruption was checked by PCR (Fig. S1B, C). All DNA fragments amplified by PCR were verified by sequencing. The oligonucleotides that were used for plasmid construction and genotyping are summarized in Tables S2 and S3.

2.4. Characterization of the fsa gene deletion mutants

For the metabolite production analysis, freshly harvested spore suspensions were inoculated in potato dextrose broth (PDB) medium. The fungal strain was cultured at 28 °C and extracted with ethyl acetate (EtOAc). The dried extracts were dissolved in methanol and analyzed by liquid chromatography/electrospray ionization mass spectrometry (LC/ESI-MS). The conditions for LC/ESI-MS and multiple reaction monitoring (MRM) analysis are described in the Supplementary methods.

For expression analysis, total RNAs were isolated from the mycelia of the *fsa* gene deletion mutants and the wild-type strain by using the RNeasy Plant Mini kit (Qiagen). One microgram of total RNA treated with DNase I was used for oligo(dT) primed cDNA synthesis using SuperScript III First Strand Synthesis System for RT-PCR (Life Technologies, Carlsbad, CA, USA) according to the manufacturer's protocols. Bio-Rad CFX96 Real-Time PCR Detection System was used for qRT-PCR, and SsoFast EvaGreen Supermix (Bio-Rad, Hercules, CA, USA) was used for cDNA amplification and detection. The primer pairs used for qRT-PCR are listed in Table S4.

2.5. Isolation of **1** and (3S,6R)-diastereomer of **1** (**3**)

Fusarium sp. FN080326 was cultured at 28 °C for 7 days in PDB medium. The fungal cultures were filtered and extracted with EtOAc. From the dried extracts, **1** was purified by silica gel chromatography, followed by preparative HPLC. Compound **2** was also isolated as described previously [10]. Structures of **1** and **2** were identified as equisetin [14] and fusarisetin A [10] by comparison of their physicochemical properties and NMR data, including 2D NMR spectra.

For the isolation of **3**, the Δ*fsa2* strain derived from FN080326 was cultured at 28 °C for 2 weeks in PDB medium. The whole culture broth (14 L) was extracted 3 times with a half volume of EtOAc. It was evaporated to yield 1.02 g of crude extract. The EtOAc extract was separated into 8 fractions by SiO_2 medium pressure liquid chromatography (MPLC), with a stepwise gradient of $CHCl_3$/MeOH. The first fraction eluted with 100% of $CHCl_3$ was further separated by SiO_2 MPLC with a linear gradient of hexane/EtOAc to afford 5 fractions. The 2nd fraction, showing 2 peaks with the same *m*/*z* value of 374 $[M+H]^+$ in LC/MS analysis, was again separated by SiO_2 MPLC with a linear gradient of hexane/EtOAc to give crude fractions of compounds **3** and **1** as the 2nd and 4th fraction, respectively. Each fraction was purified by C_{18}- HPLC with isocratic elution of MeOH/0.05% aqueous formic acid (8:2) to afford **3** (10.2 mg) and **1** (5.3 mg) as colorless amorphous solids. The physicochemical properties and ^1H and ^{13}C NMR spectra of **3** are summarized in the Supplementary Information (Tables S5 and S6, and Fig. S2–S8). The physicochemical properties of **1** were identical to the data obtained from the compound extracted from the wild-type culture described above.

3. Results

3.1. Identification of the biosynthesis gene cluster for **1** and **2** in *Fusarium* sp. FN080326

To explore secondary metabolite biosynthetic gene clusters of the producer strain of **2**, the genome of the strain FN080326 was sequenced using Illumina 100-bp paired end sequencing. Sequence analysis showed that the genome harbored a number of PKS and NRPS genes like most filamentous fungi, but fortunately, only one PKS-NRPS hybrid gene, *fsa1*, was found in the genome (Table S1). Enzymatic genes that were likely to be involved in the biosynthesis of **1**, such as those encoding *trans*-acting enoyl reductase (ER) domain protein and methyltransferase as well as $Zn(II)_2Cys_6$ (C6)-type transcription factor genes, were adjacent to *fsa1* (Fig. 1). Features of the gene products in the *fsa* cluster and its neighbors are summarized in Table 1 (GenBank: LC025956). The biosynthetic gene (*eqx*) cluster of **1** in *Fusarium heterosporum* ATCC 74349, which has been corrected recently [15], was very similar to the *fsa* cluster (Table 1).

Knockout experiments were carried out to demonstrate that the *fsa* gene cluster is involved in the biosynthesis of **1** in the fungal strain FN080326. Gene deletion mutants were generated by replacing the entire coding region of the *fsa* gene by the hygromycin B-resistance gene cassette (Fig. S1). Metabolite

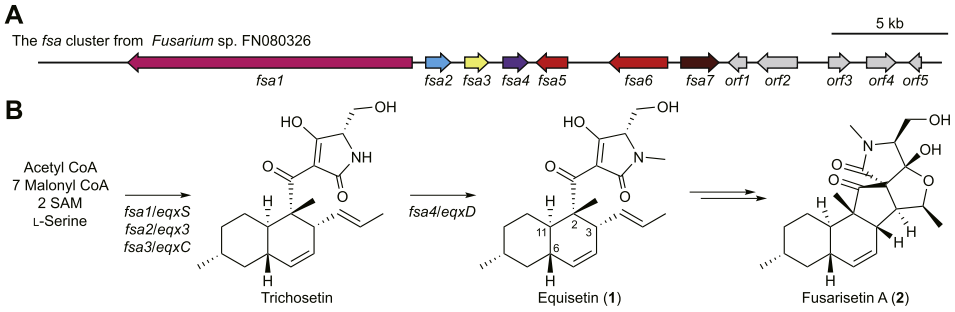

Fig. 1. The biosynthetic gene (*fsa*) cluster (A) and the proposed biosynthetic pathway (B) of equisetin (**1**) and fusarisetin A (**2**) in *Fusarium* sp. FN080326.

profiles of the deletion mutants were determined by LC/ESI-MS. The *fsa1* deletion resulted in the loss of production of **1** and **2** (Fig. 2A and B). Feeding **1** to the culture of the *fsa1* deletion mutant restored the production of **2** (Fig. 2B). These results clearly showed that **2** was converted from **1** and that its production required the gene cluster containing *fsa1*.

3.2. Involvement of *fsa2* in the stereocontrolled decalin formation of **1**

The functions of Fsa2 in the biosynthesis of **1** had not been predicted because Fsa2 did not show homology to any known proteins or functional motifs. In addition to a significant decrease in the production of **1**, a new peak with the same *m*/*z* value of 374 $[M+H]^+$ as that of **1** was detected in the Δ*fsa2* mutant (Fig. 2A inset). Compounds from these two peaks were isolated from the culture broth of the Δ*fsa2* mutant. A compound corresponding to the peak eluted later was identified as **1** by mass spectroscopy and NMR measurements. High resolution ESI-MS revealed that the other compound had the same molecular formula as that of **1**, $C_{22}H_{32}NO_4$. Its structure was determined as (3*S*,6*R*)-diastereomer of **1** (**3**) based on 2D NMR correlations in HH-COSY (Fig. S5), HSQC (Fig. S6), and HMBC spectra (Fig. S7) and the comparison of NMR chemical shift values with those of **1** (Fig. 3A, Table S6). The stereochemistry of the treramic acid moiety of **3** was found to be the same as that of **1** because their NMR chemical shift values were in good agreement with each other [14]. The relative stereochemistry for the decalin ring of **3** was determined to be a *cis*-conformation by the correlation in phase-sensitive NOESY spectra (Fig. S8), which showed NOESY correlations between H-6 and H-11, between H-10ax and H-13, between H_3-12 and three of H-10eq, H-11, and H-13, and between H-5 and both of H-7eq and H-8, which assigned the methyl group at C-8 as equatorial (Fig. 3B). These correlations also assigned the configurations of C-2 of **3**, which were same as those of **1**. The optical rotation ($[\alpha]^{24}_{589}$ +158°) and the CD spectrum ($\Delta\varepsilon$ $+3.1_{260}$) were opposite in sign to those of **1** ($[\alpha]^{24}_{589}$ −294°, $\Delta\varepsilon$ -2.3_{260}). Related *cis*- and *trans*-decalin analogues, pyrrolocins B and C, showed a similar change in the measurement of optical rotation and CD spectra [16]. These observations suggested that the absolute configuration for the decalin moiety of **3** was 2*S*, 3*S*, 6*R*, 8*R*, 11*R*, and 5′*S*. Therefore, *fsa2* is responsible for the stereocontrol at C-3 and C-6 positions among the stereocenters forged in the [4+2] cycloaddition, i.e., it functions as an *endo*-selective Diels-Alderase in the decalin formation of **1** (Fig. 3C).

3.3. **1** and **2** biosynthetic pathway in *Fusarium* sp. FN080326

To determine the roles of *fsa* genes in the biosynthesis of **1** and **2**, targeted gene inactivation was performed with the other *fsa* genes as well as neighboring genes from *orf1* to *orf5*. No production of **1** and **2** was detected in the *fsa3* and *fsa4* deletion mutants (*fsa3* and *fsa4* encode a *trans*-ER and methyltransferase, respectively). Instead, a peak with an *m*/*z* of 360 $[M+H]^+$, corresponding to a desmethyl analogue of **1**, was detected in the Δ*fsa4* mutant (Fig. S9). These observations can be explained by the predicted function of Fsa3 and Fsa4. Fsa3 cooperates with Fsa1 as a part of the megasynthase for **1** and Fsa4 catalyzes the *N*-methylation of the released product from the megasynthase (Fig. 1B). Deletion of *fsa5*, which encodes a C6-type transcriptional activator, also resulted in the loss of **1** and **2** production. Gene expression of *fsa1* and the neighboring genes, *fsa2* to *fsa5*, was undetectable in the Δ*fsa5* mutant (Fig. S10), indicating that *fsa5* encodes the pathway-specific transcriptional

Table 1
Features of the *fsa* gene products of *Fusarium* sp. FN080326.

Gene	Size (bp/aa)	Deduced function[a]	Relatives (accession, identity[%])[b]	Production of **1** in the deletion mutant[c]
fsa1	12267/3949	PKS-NRPS hybrid*	EqxS (AGO86662, 93), PrlS (AIP87510, 51)	−
fsa2	1125/375	Diels-Alderase*	Eqx3 (AGO86663, 90), gNR600 (AIP87501, 37)	±
fsa3	1062/354	*trans*-acting ER*	EqxC (AGO86659, 97), PrlC (AIP87505, 60)	−
fsa4	1126/360	MT*	EqxD (AGO86665, 93), GsfC from *Penicillium aethiopicum* (ADI24955, 28)	−
fsa5	1398/466	C6TF*	EqxR (AGO86667, 88), LovE from *Aspergillus terreus* (AAD34557, 37)	−
fsa6	2459/739	C6TF	EqxF (AGO86660, 84), PrlR (AIP87509, 42)	+
fsa7	1681/508	MFS transporter	EqxG (AGO86666, 91), PrlG (AIP87507, 60)	+
orf1	825/275	vWA-like protein	Eqx9 (AGO86669, 97)	++
orf2	1820/533	Cytochrome P450	EqxH (AGO86661, 88), GA20 oxidase from *F. fujikuroi* (CAA75566, 42)	++
orf3	964/304	SDR family protein	Eqx11 (AGO86664, N-terminal, 87)	++
orf4	1277/353	Unknown	Eqx11 (AGO86664, C-terminal, 72)	++
orf5	576/191	Cell wall protein	alkaline foam protein A AfpA from *F. culmorum* (ABC61860, 41)	++

Abbreviation: MT, methyltransferase; C6TF, C6 transcription factor; MFS, major facilitator superfamily; vWA, von Willebrand factor type A; SDR, short-chain dehydrogenases/reductases.

[a] Asterisks indicate functions confirmed genetically in this study.

[b] Homologous proteins listed are those whose functions are characterized and/or those involved in the known biosynthetic pathways.

[c] Production of **1** in the respective gene deletion mutants: ++, comparable to WT; +, approximately 10% of WT; ±, <1% of WT; −, not detected.

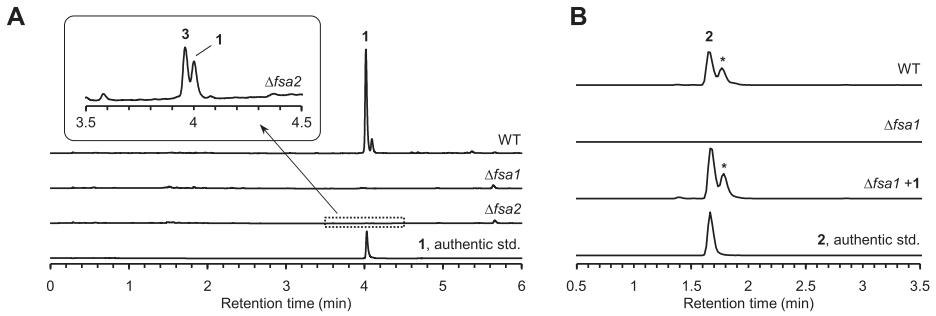

Fig. 2. Characterization of the *fsa* gene deletion mutants (A) Metabolite profile of the wild-type (WT), Δ*fsa1*, and Δ*fsa2* strains. The fungal strains were cultured at 28 °C for 14 days. The culture extracts were analyzed by LC/ESI-MS. UV detection was carried out at 294 nm. The production was tested independently in more than 5 strains of the Δ*fsa1* and the Δ*fsa2* mutants. Inset magnified UV chromatogram shows the production of **1** and the *cis*-decalin analogue **3** in the Δ*fsa2* mutant. (B) Feeding experiments with **1** in the Δ*fsa1* mutant. The fungal strains were precultured at 28 °C for 3 days and **1** was added into the cultures at a final concentration of 20 μg/mL. The cultures were further incubated at 28 °C for 6 days. The culture extracts were analyzed by LC/ESI-MS. MRM analysis was performed for the detection of **2**. The peak indicated with an asterisk was an unidentified product converted from **1**, showing the same *m*/*z* value as that of **2**.

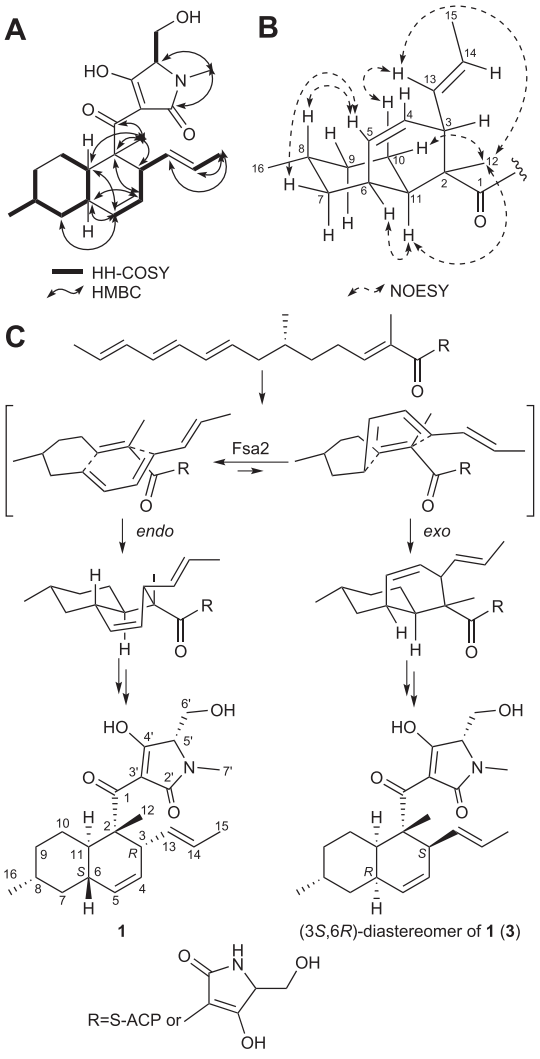

Fig. 3. Structural determination of **3** and the proposed function of Fsa2 as a Diels-Alderase (A) HH-COSY and HMBC correlations for the planner structure. (B) NOESY correlations for the relative stereochemistry. (C) Putative mechanism of decalin formation involving Fsa2 in the biosynthesis of **1**. In addition to the inherent product **1**, the *cis*-decalin analogue **3** was detected in the Δ*fsa2* mutant of *Fusarium* sp. FN080326. Whether the actual substrate of the reaction is an enzyme-tethered intermediate or a released tetramic acid remains to be determined.

activator of the *fsa* cluster and that its deletion caused an inactivation of the *fsa* genes, resulting in the loss of production. In contrast, the expression of the *fsa* genes was decreased, but could be still observed in the *fsa6* deletion mutant, which also encodes a C6-type transcription factor (Fig. S10), suggesting that *fsa6* could play a secondary role in the regulation of the *fsa* cluster in this fungus.

The production of **1** and **2** was fairly reduced in the Δ*fsa6* and Δ*fsa7* mutants, whereas no effect of the gene deletion on the production was observed in the *orf1* to *orf5* deletion mutants (Table 1). The upstream region of *fsa1*, which was 3.8 kb in length from the stop codon of *fsa1* to the contig end, appeared to contain no ORF. Although a part of the sequence showed homology to the gene annotated as *eqx1* in the *F. heterosporum* genome, the transcript level from the orthologous region of *eqx1* was below the detection limit. Taken together, we proposed that the *fsa* cluster consists of 7 genes, *fsa1* to *fsa7*, which are responsible for the biosynthesis of **1** in the *Fusarium* sp. FN080326 (Fig. 1).

4. Discussion

Our genetic analysis clearly showed that the *fsa* cluster was responsible for the biosynthesis of **1**, which was further converted to **2** in *Fusarium* sp. FN080326. Knockout experiments were carried out for 11 genes located downstream of *fsa1* and their involvement in the biosynthesis of **1** and **2** was evaluated. Analysis of the deletion mutants allowed us to determine the roles of five *fsa* genes, *fsa1* to *fsa5*, in the biosynthesis of **1** in the strain FN080326 (Fig. 1B). Unexpectedly, we found a new function for *fsa2*, which had been unannotated due to a lack of homologous protein folds or sequences, in the biosynthesis of **1**. Production of **1** as well as the *cis*-decalin analogue **3** in the Δ*fsa2* mutant indicated that *fsa2* is involved in *endo*-selective Diels-Alder cycloaddition to form the decalin ring of **1**.

The decalin ring found in the fungal tetramic acids can be divided into 4 groups according to their stereochemistry (Fig. S11). There has been no report on the isolation of metabolites with different stereochemistry in the decalin moiety from a single strain, pointing to the existence of mechanism(s) to strictly control the stereochemistry in decalin formation. Very recently, the pyrrolocin biosynthetic gene (*prl*) cluster has been identified [17]. The gene organization of the *prl* cluster is similar to those of the *fsa* and *eqx* cluster, which include a PKS-NRPS hybrid gene, *prlS*, a *trans*-ER gene, *prlC*, and the *fsa2* orthologue, *gNR600* (Fig. 4). While only pyrrolocin A, presenting a *trans*-decalin ring, was isolated from the fungal strain NRRL 50135, both the *cis*- and *trans*-decalin analogues,

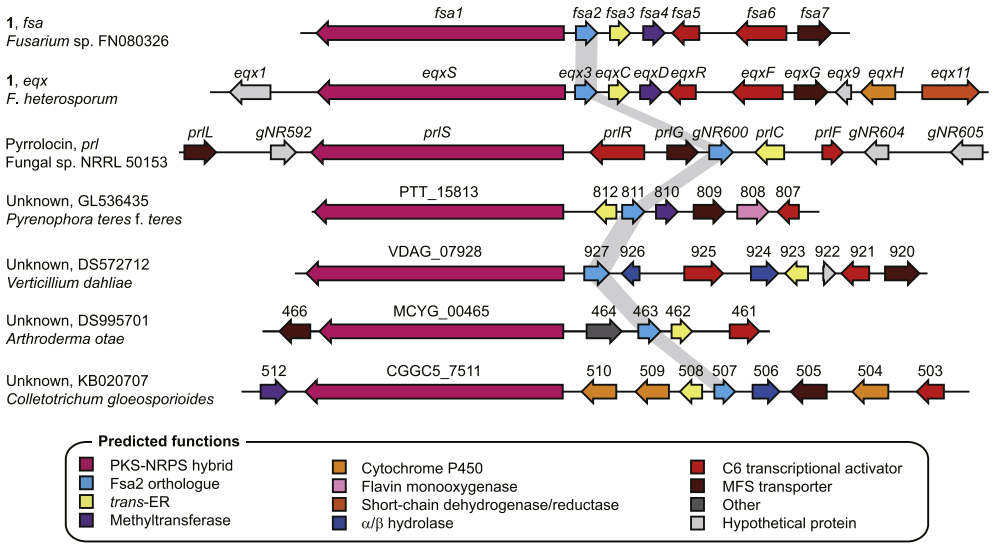

Fig. 4. Comparison of the biosynthetic gene clusters for **1** (*fsa*, *eqx*) and pyrrolocin (*prl*), with putative gene clusters for fungal metabolites possibly containing a decalin ring. More than 50 gene clusters containing a PKS-NRPS hybrid, a *trans*-ER, and a *fsa2* orthologous genes were found in the database. Some representative gene clusters used for the comparison are as followed: the *fsa* genes from *Fusarium* sp. FN080326, the *eqx* genes from *Fusarium heterosporum* ATCC 74349 (GenBank: KC439347), the *prl* genes from the fungal sp. NRRL 50135 (KM107910), PTT_15807 to 813 from *Pyrenophora teres* f. *teres* 0-1 (GL536435), VDAG_07920 to 28 from *Verticillium dahliae* VdLs.17 (DS572712), MCYG_00461 to 466 from *Arthroderma otae* CBS 113480 (DS995701), and CGGC5_7503 to 7512 from *Colletotrichum gloeosporioides* Nara gc5 (KB020707).

pyrrolocin B and C, were produced in a heterologous expression host that carries *prlS* and *prlC* [16,17]. This observation is consistent with our findings and strongly supports the idea that Fsa2 is a new enzyme involved in the stereoselective formation of the decalin ring of **1**.

Although a number of fungal tetramic acids containing a decalin ring have been isolated because of their various biological activities [10,18–23], only a few biosynthetic gene clusters have been identified. Most of the *fsa2* orthologues found in the database are located adjacent to the PKS-NRPS hybrid and *trans*-ER genes (Fig. 4). Whether the Fsa2 function is commonly used in the biosynthetic pathways of decalin-containing metabolites should be further studied.

Contrary to our prediction, no deletion mutant was obtained, in which the production of **2**, but not **1**, was lost, implying that an enzymatic gene responsible for the conversion should be located outside of the *fsa* cluster. Involvements of factors outside gene clusters have been shown in the biosynthetic pathways of fumitremorgin A, nidulanin A, and spirotryprostatins [24–26]. A genome-wide survey based on bioinformatics and transcriptome analysis will provide information allowing us to identify the biosynthetic pathway of **2**.

In summary, we identified the *fsa* cluster for the biosynthesis of **1** from *Fusarium* sp. FN080326 and showed that fused pentacyclic compound **2** was formed from **1**. Our genetic analysis and following structural elucidation of metabolites unveiled a new enzyme involved in the stereochemical outcome in the [4 + 2] cycloaddition to form a decalin scaffold in the fungal PKS-NRPS hybrid pathway. Biochemical characterization of Fsa2 as well as demonstration of the Fsa2 function in biosynthetic pathways of fungal tetramic acids, containing a *cis*-decalin such as pyrrolizilactone [23], will lead to further exploration of the structural diversity in this class of compounds.

Conflict of interest

None.

Acknowledgments

We are grateful to Dr. J. Ishikawa for the prediction of the secondary metabolite biosynthetic gene cluster, Dr. Y. Hongo for high resolution ESI-MS measurements, Dr. M. Ueki for compound preparation, and K. Kinugasa and A. Okano for technical assistance. We also thank GeNAS for genome sequence data production. This work was supported by Grants-in-Aid for Scientific Research from the Japan Society for the Promotion of Science, the science and technology research promotion program for agriculture, forestry, fisheries and food industry, grants from the Global R&D Center (GRDC, NRF-2010-00719) programs of the National Research Foundation of Korea funded by the Ministry of Science, ICT and Future Planning of Korea (MSIFP) and a grants from the KRIBB Research Initiative Program.

Appendix A. Supplementary data

Supplementary data related to this article can be found at http://dx.doi.org/10.1016/j.bbrc.2015.03.011.

Transparency document

Transparency document related to this article can be found online at http://dx.doi.org/10.1016/j.bbrc.2015.03.011.

References

[1] Y.H. Chooi, Y. Tang, Navigating the fungal polyketide chemical space: from genes to molecules, J. Org. Chem. 77 (2012) 9933–9953.
[2] D. Boettger, C. Hertweck, Molecular diversity sculpted by fungal PKS-NRPS hybrids, Chembiochem 14 (2013) 28–42.
[3] E.M. Stocking, R.M. Williams, Chemistry and biology of biosynthetic Diels-Alder reactions, Angew. Chem. Int. Ed. Engl. 42 (2003) 3078–3115.
[4] H. Oikawa, T. Tokiwano, Enzymatic catalysis of the Diels-Alder reaction in the biosynthesis of natural products, Nat. Prod. Rep. 21 (2004) 321–352.
[5] C.D. Campbell, J.C. Vederas, Biosynthesis of lovastatin and related metabolites formed by fungal iterative PKS enzymes, Biopolymers 93 (2010) 755–763.

[6] S.G. Brown, M.J. Jansma, T.R. Hoye, Case study of empirical and computational chemical shift analyses: reassignment of the relative configuration of phomopsichalasin to that of diaporthichalasin, J. Nat. Prod. 75 (2012) 1326–1331.
[7] K. Auclair, A. Sutherland, J. Kennedy, D.J. Witter, J.P. Van den Heever, C.R. Hutchinson, J.C. Vederas, Lovastatin nonaketide synthase catalyzes an intramolecular Diels-Alder reaction of a substrate analogue, J. Am. Chem. Soc. 122 (2000) 11519–11520.
[8] K. Kasahara, T. Miyamoto, T. Fujimoto, H. Oguri, T. Tokiwano, H. Oikawa, Y. Ebizuka, I. Fujii, Solanapyrone synthase, a possible Diels-Alderase and iterative type I polyketide synthase encoded in a biosynthetic gene cluster from *Alternaria solani*, Chembiochem 11 (2010) 1245–1252.
[9] J. Kennedy, K. Auclair, S.G. Kendrew, C. Park, J.C. Vederas, C.R. Hutchinson, Modulation of polyketide synthase activity by accessory proteins during lovastatin biosynthesis, Science 284 (1999) 1368–1372.
[10] J.H. Jang, Y. Asami, J.P. Jang, S.O. Kim, D.O. Moon, K.S. Shin, D. Hashizume, M. Muroi, T. Saito, H. Oh, B.Y. Kim, H. Osada, J.S. Ahn, Fusarisetin A, an acinar morphogenesis inhibitor from a soil fungus, *Fusarium* sp. FN080326, J. Am. Chem. Soc. 133 (2011) 6865–6867.
[11] J. Xu, E.J. Caro-Diaz, L. Trzoss, E.A. Theodorakis, Nature-inspired total synthesis of (-)-fusarisetin A, J. Am. Chem. Soc. 134 (2012) 5072–5075.
[12] N. Kato, H. Suzuki, H. Takagi, Y. Asami, H. Kakeya, M. Uramoto, T. Usui, S. Takahashi, Y. Sugimoto, H. Osada, Identification of cytochrome P450s required for fumitremorgin biosynthesis in *Aspergillus fumigatus*, Chembiochem 10 (2009) 920–928.
[13] T. Motoyama, T. Hayashi, H. Hirota, M. Ueki, H. Osada, Terpendole E, a kinesin Eg5 inhibitor, is a key biosynthetic intermediate of indole-diterpenes in the producing fungus *Chaunopycnis alba*, Chem. Biol. 19 (2012) 1611–1619.
[14] N.J. Phillips, J.T. Goodwin, A. Fraiman, R.J. Cole, D.G. Lynn, Characterization of the *Fusarium* toxin equisetin - the use of phenylboronates in structure assignment, J. Am. Chem. Soc. 111 (1989) 8223–8231.
[15] T.B. Kakule, D. Sardar, Z. Lin, E.W. Schmidt, Two related pyrrolidinedione synthetase loci in *Fusarium heterosporum* ATCC 74349 produce divergent metabolites, ACS Chem. Biol. 8 (2013) 1549–1557.
[16] R.C. Jadulco, M. Koch, T.B. Kakule, E.W. Schmidt, A. Orendt, H. He, J.E. Janso, G.T. Carter, E.C. Larson, C. Pond, T.K. Matainaho, L.R. Barrows, Isolation of pyrrolocins A-C: *cis*- and *trans*-decalin tetramic acid antibiotics from an endophytic fungal-derived pathway, J. Nat. Prod. 77 (2014) 2537–2544.
[17] T.B. Kakule, R.C. Jadulco, M. Koch, J.E. Janso, L.R. Barrows, E.W. Schmidt, Native promoter strategy for high-yielding synthesis and engineering of fungal secondary metabolites, ACS Synth. Biol. (2015), http://dx.doi.org/10.1021/sb500296p in press.
[18] R.F. Vesonder, L.W. Tjarks, W.K. Rohwedder, H.R. Burmeister, J.A. Laugal, Equisetin, an antibiotic from *Fusarium equiseti* NRRL 5537, identified as a derivative of *N*-methyl-2,4-pyrollidone, J. Antibiot. 32 (1979) 759–761.
[19] S.B. Singh, D.L. Zink, M.A. Goetz, A.W. Dombrowski, J.D. Polishook, D.J. Hazuda, Equisetin and a novel opposite stereochemical homolog phomasetin, two fungal metabolites as inhibitors of HIV-1 integrase, Tetrahedron Lett. 39 (1998) 2243–2246.
[20] Y. Sugie, S. Inagaki, Y. Kato, H. Nishida, C.H. Pang, T. Saito, S. Sakemi, F. Dib-Hajj, J.P. Mueller, J. Sutcliffe, Y. Kojima, CJ-21,058, a new SecA inhibitor isolated from a fungus, J. Antibiot. 55 (2002) 25–29.
[21] N. Koyama, T. Nagahiro, Y. Yamaguchi, T. Ohshiro, R. Masuma, H. Tomoda, S. Omura, Spylidone, a novel inhibitor of lipid droplet accumulation in mouse macrophages produced by *Phoma* sp. FKI-1840, J. Antibiot. 58 (2005) 338–345.
[22] J. Inokoshi, N. Shigeta, T. Fukuda, R. Uchida, K. Nonaka, R. Masuma, H. Tomoda, *Epi*-trichosetin, a new undecaprenyl pyrophosphate synthase inhibitor, produced by *Fusarium oxysporum* FKI-4553, J. Antibiot. 66 (2013) 549–554.
[23] T. Nogawa, M. Kawatani, M. Uramoto, A. Okano, H. Aono, Y. Futamura, H. Koshino, S. Takahashi, H. Osada, Pyrrolizilactone, a new pyrrolizidinone metabolite produced by a fungus, J. Antibiot. 66 (2013) 621–623.
[24] K. Mundt, B. Wollinsky, H.L. Ruan, T. Zhu, S.M. Li, Identification of the verruculogen prenyltransferase FtmPT3 by a combination of chemical, bioinformatic and biochemical approaches, Chembiochem 13 (2012) 2583–2592.
[25] M.R. Andersen, J.B. Nielsen, A. Klitgaard, L.M. Petersen, M. Zachariasen, T.J. Hansen, L.H. Blicher, C.H. Gotfredsen, T.O. Larsen, K.F. Nielsen, U.H. Mortensen, Accurate prediction of secondary metabolite gene clusters in filamentous fungi, Proc. Natl. Acad. Sci. U. S. A. 110 (2013) E99–E107.
[26] Y. Tsunematsu, N. Ishikawa, D. Wakana, Y. Goda, H. Noguchi, H. Moriya, K. Hotta, K. Watanabe, Distinct mechanisms for spiro-carbon formation reveal biosynthetic pathway crosstalk, Nat. Chem. Biol. 9 (2013) 818–825.